

Research Article

Solid-Phase Preparation of Al-TiO₂ for Efficient Separation of Bioderived Product Danshensu

Fei Chang ¹, Zhong Bing He,¹ and Quan Zhou²

¹Institute of Comprehensive Utilization of Plant Resources, Kaili College, Kaili 556011, China

²Pharmaceutical and Bioengineering College, Hunan Chemical Vocational Technology College, Zhuzhou, Hunan 412000, China

Correspondence should be addressed to Fei Chang; feichang1980@126.com

Received 2 June 2019; Revised 22 July 2019; Accepted 14 September 2019; Published 3 November 2019

Academic Editor: Dimosthenis L. Giokas

Copyright © 2019 Fei Chang et al. This is an open access article distributed under the Creative Commons Attribution License, which permits unrestricted use, distribution, and reproduction in any medium, provided the original work is properly cited.

Four kinds of Al-TiO₂ solid samples with different Ti/Al ratios of 1 : 0.1, 1 : 0.09, 1 : 0.07, and 1 : 0.05 were synthesized via a solid-phase synthesis method and characterized by XRD, SEM, EDS, BET, and other techniques. The prepared solids were used for separation of the bioderived product danshensu, the content of which was determined by UV spectrophotometry. Moreover, the effects of extract concentration, pH value, adsorption time, and ethanol elution volume were investigated. The results showed that these Al-TiO₂ samples had good adsorption and desorption ability. Especially, the solid Al-TiO₂ with a Ti/Al ratio of 1 : 0.05 is more suitable for the separation of danshensu, exhibiting a higher adsorption (77.70%) under 2 h adsorption time and pH = 3; meanwhile, the high desorption rate (70.29%) was received under 80% ethanol and the sample concentration of 3.0 mg/mL.

1. Introduction

Danshensu significantly inhibits the growth of cancer cells and makes the tk/GCV (herpes simplex virus thymidine kinase/ganciclovir) system of cancer cells enhance the synergistic effect of killing and the effect of suicide gene bystanders (BE) [1]. The previous study also found that danshensu can significantly inhibit the rise of blood lipids in rabbits with a high-fat diet and can also inhibit the synthesis of endogenous cholesterol cells [2]. In the field of medicine, danshensu has a more broad application prospect. Therefore, the effective separation and purification of danshen sodium SSH (*Salvia scapiformis* Hance) on the full development and utilization of white tonic has great significance.

Salvia miltiorrhiza separation often uses the extraction or alcohol precipitation method [3–6], but there are bottlenecks such as separation difficulties and serious pollution problems of science and technology. In recent years, with the in-depth study of TiO₂ powder material, it was found that it not only has the basic characteristics of common materials but also has adjustable pore size, narrow pore size distribution, ordered structure, and larger specific surface area with a certain choice of adsorption properties and adsorption capacity [7] because

of which it is widely used in the adsorption and separation of organic matter and metal ions [8]. Thus, the synthesis and properties of powder materials research and development have become the current focus of materials chemistry, physics, and traditional Chinese medicine and other disciplines [9–12], so as to achieve the powder material and drug substance molecules surface atoms or active sites selective adsorption [13].

In this study, the Al-TiO₂ samples were prepared by the solid-phase synthesis method for the first time. According to the different doping amounts, different adsorbent materials were obtained, and the influencing factors on the static adsorption of danshensu in SSH were studied by the concentration of extract, pH value, adsorption time, and elution volume fraction of ethanol. It provided a scientific theoretical basis for the effective development and utilization of this plant.

2. Experiments

2.1. Materials. Danshensu (HPLC ≥ 98%, Figure 1) standard was purchased from Beijing Solarbio Technology Co., Ltd.; tetrabutyl titanate (TBOT, 98%), hydrochloric acid (HCl),

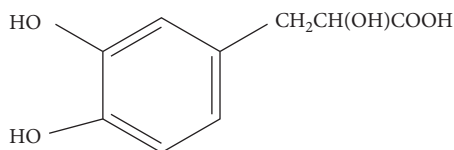


FIGURE 1: Chemical structure of danshensu.

sodium hydroxide barium chloride (BaCl_2), aluminum sulfate octadecanoate ($\text{Al}_2(\text{SO}_4)_3 \cdot 18\text{H}_2\text{O}$), cetyltrimethylammonium bromide (CTAB), anhydrous ethanol, and petroleum ether are analytical grade and purchased from Shanghai Aladdin Bio-Chem Technology Co., Ltd.

2.2. Preparation of Al-TiO_2 . $\text{Al}_2(\text{SO}_4)_3 \cdot 18\text{H}_2\text{O}$ with a Ti/Al molar ratio of 1/0.1, 1/0.09, 1/0.07, and 1/0.05 was mixed with an appropriate amount of CTAB (20 wt.% of the total amount of $\text{Al}_2(\text{SO}_4)_3 \cdot 18\text{H}_2\text{O}$ and TBOT) and ground for 25 min in a mortar. Then, 3.403 g TBOT was added to the above mixture and was continuously ground for 20 min. After static standing for 6 h at room temperature, the reactor was transferred into 140°C muffle furnace for 2 h to obtain a white solid, followed by grinding with mortar and washing using a Brinell funnel with distilled water until no SO_4^{2-} (0.1 mol/L BaCl_2 solution test to determine). The resulting sample was dried at 110°C for 2 h and then placed into the muffle furnace at $1^\circ\text{C}/\text{min}$ heating rate to 550°C for 6 h. The obtained product was cooled down to the room temperature to give Al-TiO_2 .

2.3. Characterization of Al-TiO_2 . XRD patterns were measured with the Bruker D8 advanced X-ray diffractometer (XRD) with Cu $K\alpha$ radiation ($\lambda = 0.154 \text{ nm}$) at 40 kV and 30 mA with a step size of 0.02. The SEM and EDS characterizations of the catalysts were studied using the S-3400H (Shimadzu) type scanning electron microscope (SEM). The Brunauer–Emmett–Teller (BET) surface areas were measured using the N_2 adsorption/desorption apparatus (Micromeritics ASAP 2460), and the pore size and pore volume distributions were calculated using the Barrett–Joyner–Halenda (BJH) model. FT-IR spectra were obtained using the S-65 spectrophotometer (Shimadzu). The UV-Vis spectra were recorded on the Shimadzu UV-2500 spectrophotometer.

2.4. Extraction of Danshensu. A certain amount of SSH powder was placed in a Soxhlet extractor and added petroleum ether reflow at 60°C for 12 h (defatted and bleached), petroleum ether removed by using a rotary evaporator, and dried at room temperature to obtain the solid powder. 15 g of the above powder was weighed, 50% ethanol was used as the extraction solvent ($V/m = 40:1$), and the solution was microwave extracted (power: 400 W, temperature: 40°C , and time: 5 min), filtered, and concentrated, and finally, danshensu was obtained.

2.5. Danshensu Detection. At 282 nm maximum absorption wavelength, with the concentration of danshensu as the abscissa and the absorbance as the ordinate, the linear

equation was $Y = 0.01382X - 0.00443$ with the correlation coefficient $r = 0.99961$, and the concentration of danshensu in the range of 0.01–0.05 mg/mL has a good linearity by UV-Visible spectrophotometry [14].

2.6. Danshensu Static Adsorption and Desorption Experiments. A certain concentration of danshensu solution was removed accurately into a 250 mL triangle bottle with 1.0 g Al-TiO_2 , and the appropriate time and the adsorption rate are calculated according to formula (1). Next, Al-TiO_2 was collected after adsorption, followed by putting into another triangle bottle by filtration. Ethanol was added, shaken at room temperature for 60 min, and left for 12 h. The supernatant was collected by centrifugation, the absorbance was measured by UV-Vis, and the desorption rate was calculated on the basis of formula (2).

The formula of adsorption rate calculation:

$$P_1 = \frac{(C_0V_0 - C_1V_1)}{C_0V_0} \times 100\%. \quad (1)$$

The formula of desorption rate calculation:

$$P_2 = \frac{C_2V_2}{(C_0V_0 - C_2V_2)} \times 100\%, \quad (2)$$

where P_1 : adsorption rate, P_2 : desorption rate, C_0 : danshensu solution mass concentration (mg/mL) before adsorption, V_0 : volume of danshensu solution before adsorption (mL), C_1 : danshensu mass concentration (mg/mL) after adsorption, V_1 : volume of danshensu solution after adsorption (mL), C_2 : danshensu concentration (mg/mL) after desorption, and V_2 : volume of danshensu solution (mL) after desorption.

3. Results and Discussion

3.1. Characterization of Al-TiO_2

3.1.1. EDS Characterization. In order to confirm whether the Al^{3+} is doped into TiO_2 , the four kinds of Al-TiO_2 were analyzed by EDS characterization, and the results are shown in Figure 1. As can be seen from Figure 2, all four samples are Al^{3+} -doped TiO_2 . Among them, the contents of Al in samples A and B are higher than C and D, while B has the highest in the four samples, and C and D have the same basicity. This result preliminarily showed that the adsorption rates of danshensu by A and B are higher than those by C and D because Al^{3+} is a two-type metal, and danshensu is acidic, and amount of Al^{3+} directly affects the acidity and alkalinity of Al-TiO_2 .

3.1.2. XRD. The Al-TiO_2 samples were characterized by XRD to understand the adsorption properties, and the results are shown in Figure 3. From the results, we can see that the Al-TiO_2 was prepared successfully, which is consistent with the EDS analysis. Also, with the increase of Al content, the XRD bands of Al-TiO_2 become sharper, indicating that the crystallinity of Al-TiO_2 is also increasing, leading to the permeability and compactness of Al-TiO_2 enhancement.

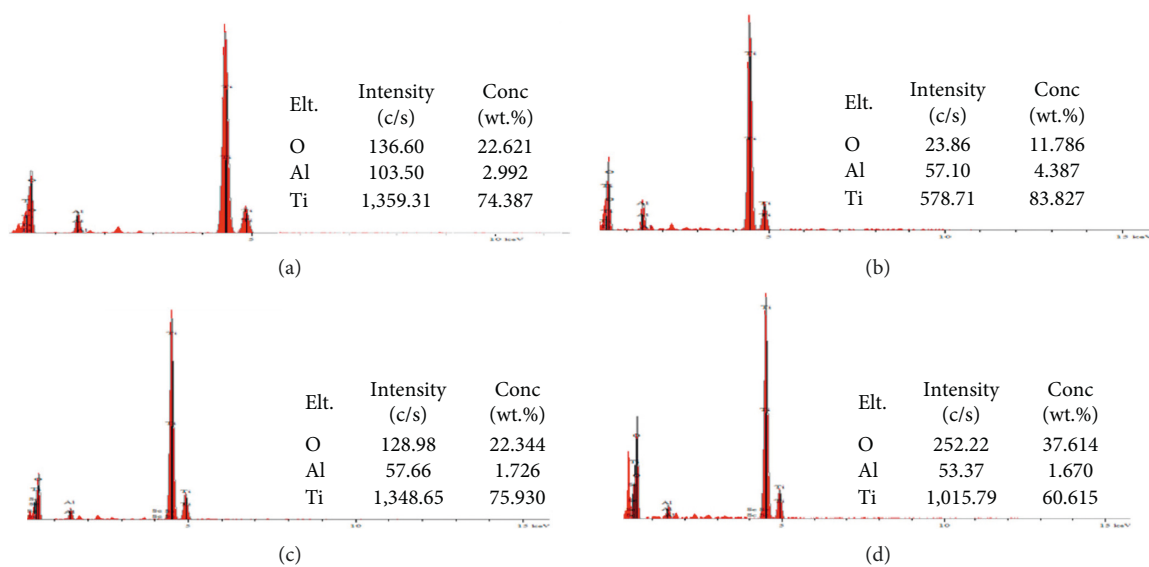


FIGURE 2: EDS analysis of Al-TiO₂ samples. (a) Ti/Al = 1:0.1; (b) Ti/Al = 1:0.09; (c) Ti/Al = 1:0.07; (d) Ti/Al = 1:0.05.

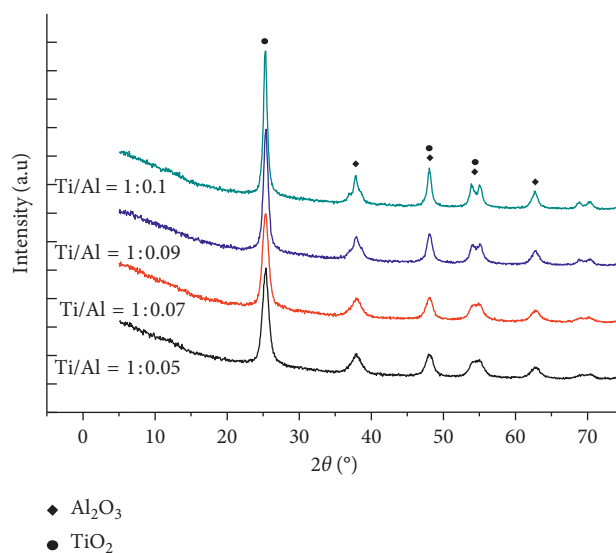


FIGURE 3: The XRD patterns of Al-TiO₂ samples.

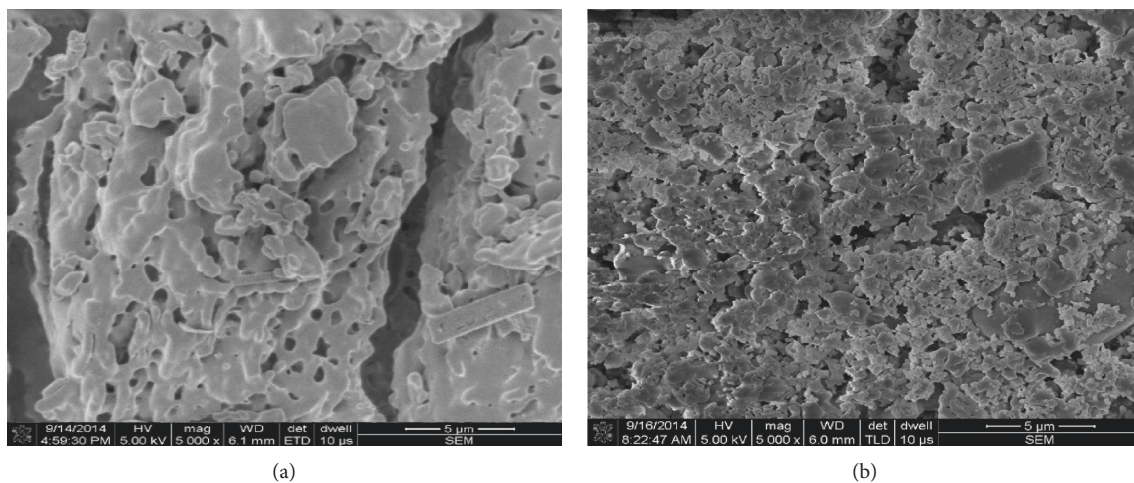


FIGURE 4: Continued.

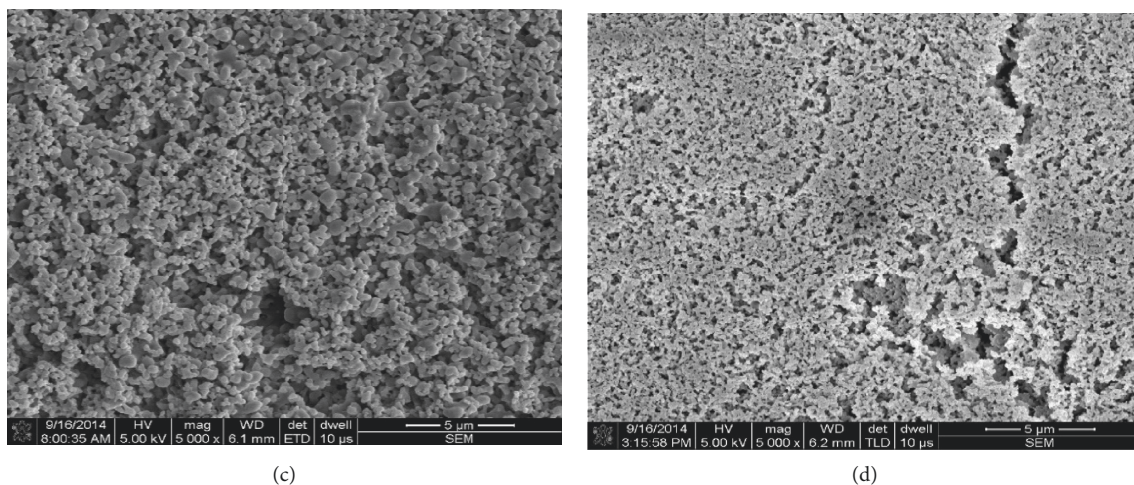


FIGURE 4: SEM images of Al-TiO₂ powders with different Ti/Al ratios. (a) Ti/Al = 1/0.1; (b) Ti/Al = 1/0.09; (c) Ti/Al = 1/0.07; (d) Ti/Al = 1/0.05.

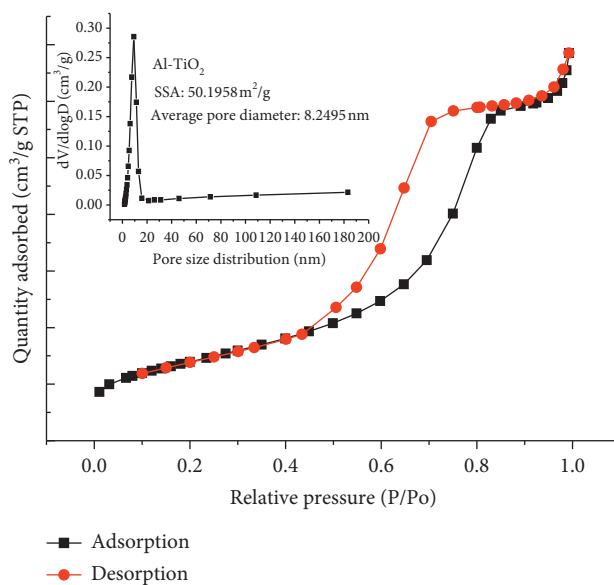


FIGURE 5: N₂ adsorption-desorption isotherms and pore size distribution of Al-TiO₂ (Ti/Al = 1/0.05).

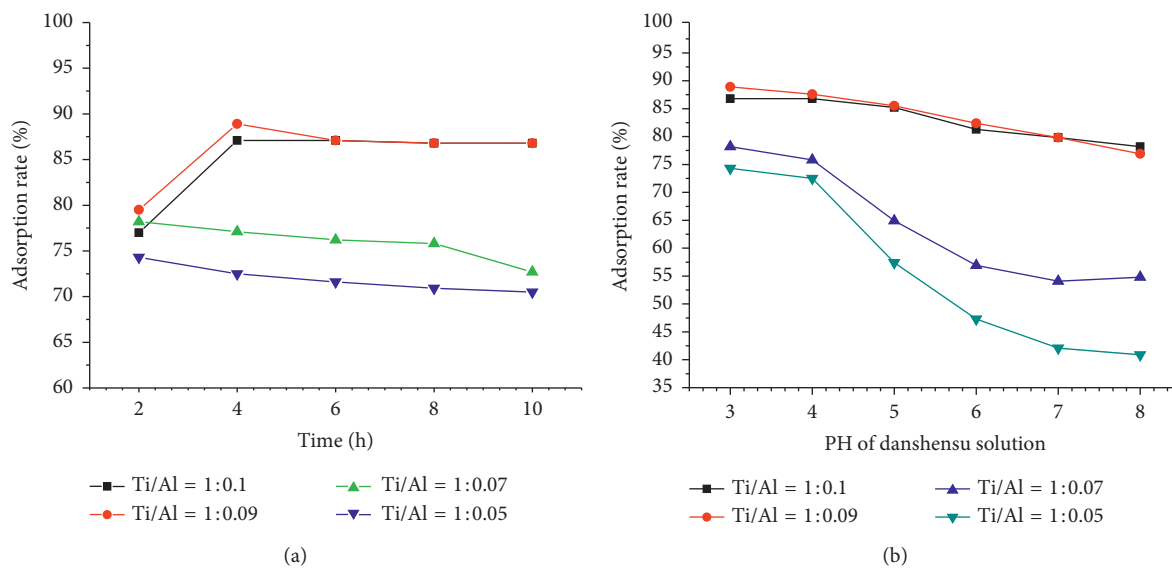


FIGURE 6: Continued.

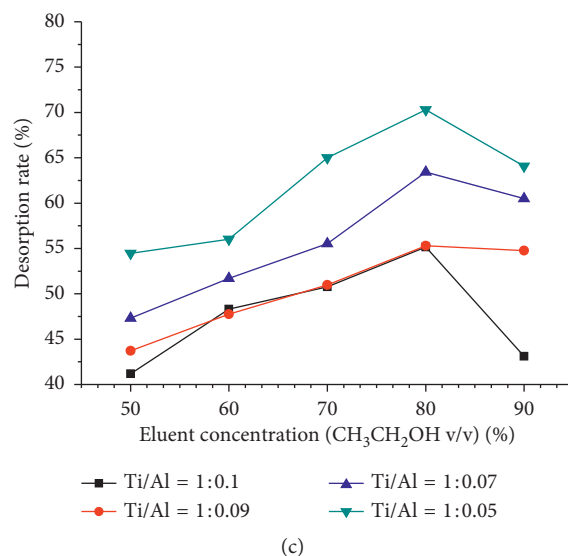
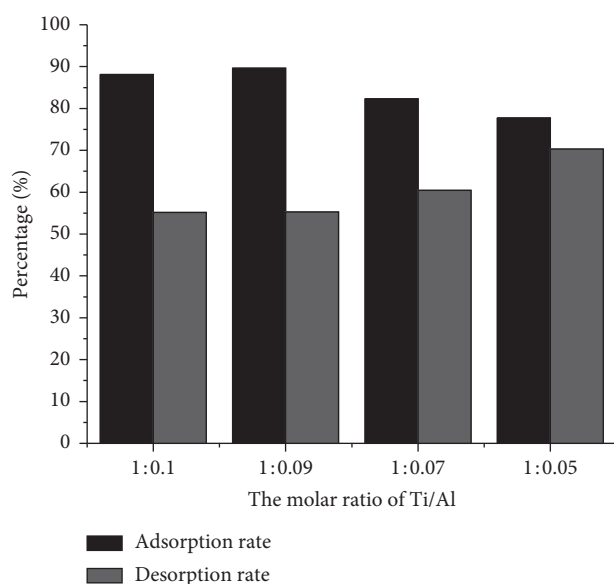


FIGURE 6: Results of adsorption and desorption condition optimization.

FIGURE 7: Results of adsorption and desorption of four Al-TiO₂ samples.

3.1.3. SEM. Material properties are closely related to their shape [15, 16], and the obtained SEM images of four different Al-TiO₂ samples are shown in Figure 4. As can be seen from Figure 4, the four Al-TiO₂ solids have a clear pore structure, but as the Al content decreases, the pore structure gradually becomes even, and the grain size of the Al-TiO₂ also decreases. In particular, Figure 4(d) is more obvious. It is preliminary judged that the four Al-TiO₂ samples have a good adsorption capacity.

3.1.4. BET. The N₂ adsorption-desorption isotherm of Al-TiO₂ (Ti/Al = 1/0.05) is shown in Figure 5. The Al-TiO₂ exhibited type IV isotherms with type H3 hysteresis loops. These observations indicated that the pores of Al-TiO₂

belong to the sheet-like stacked pores [17]. These observations were consistent with results from SEM studies. In addition, the specific surface area (SSA) of Al-TiO₂ is 50.1985 m²/g, and the average pore size is 8.2495 nm.

3.2. Optimization of Static Adsorption and Desorption Conditions. In order to obtain the best adsorption and desorption conditions of the four Al-TiO₂ samples, the adsorption time, the pH value of the danshensu solution, and the eluent concentration were investigated, respectively, and the results are shown in Figure 6. It can be seen from the results of Figures 6(a) and 6(b) that all four Al-TiO₂ materials have good adsorption capacity. Among them, the adsorption capacity of Al-TiO₂ with Ti/Al = 1/0.1 and Ti/Al = 1/0.09 are stronger than that of Ti/Al = 1/0.07 and Ti/Al = 1/0.05, and the opposite results of the desorption capacity are shown with ethanol eluent in Figure 6(c). In addition, with the time extension, the adsorption capacity also increases, but the maximum adsorption rate was reached at 4 h (Figure 6(a)), and the pH value of the danshensu solution was inversely proportional to Al-TiO₂ adsorption capacity (Figure 6(b)). In which the adsorption rate is the highest when the danshensu solution is pH = 3. At last, the result of the eluent concentration test showed that at 50–90% (v/v), the desorption rate increased with 50–80% ethanol concentration, the maximum desorption rate was received with 80% ethanol. Continuing to increase the ethanol concentration (90%), the desorption rate has a decreasing trend (Figure 6(c)), and the reason can be that danshensu was damaged by high concentrations of ethanol [18–20].

3.3. Test of Adsorption and Desorption. It can be seen from the results in Figure 7 that all four Al-TiO₂ samples have a good adsorption capacity. Among them, Al-TiO₂ with Ti/Al ratios 1/0.1 and 1/0.09 has the highest adsorption rate, but

the desorption capacity is poor. As the effective separation capability is used to measure the quality of material separation (desorption rate/adsorption rate), it can be calculated that the effective separation capability is 62.5%, 61.7%, 77.0%, and 90.3%, respectively. Thus, Al-TiO₂ with Ti/Al ratio 1/0.05 is most suitable for the separation of danshensu. The reason may be that it has a uniform pore structure [15, 21].

4. Conclusions

In conclusion, several Al-TiO₂ samples were prepared by solid-phase synthesis with TBOT and Al₂(SO₄)₃·18H₂O. Then, the optimized Al-TiO₂ was used for separation of danshensu. The experimental results showed the following:

- (1) Al-TiO₂ with Ti/Al ratios 1/0.1 and 1/0.09 has a higher adsorption rate, and the desorption rate is worse than that with Ti/Al ratios 1/0.07 and 1/0.05
- (2) The optimal conditions for isolating danshensu solution are pH = 3, 4 h adsorption time, and 80% ethanol eluent
- (3) The Al-TiO₂ sample with Ti/Al ratio 1/0.05 is the best material for separating danshensu under the best conditions

Data Availability

The data used to support the findings of this study are included within the article.

Conflicts of Interest

The authors declare that they have no conflicts of interest.

Acknowledgments

This work was financially supported by the Guizhou Provincial State University S&T Technology Joint Fund Program (Nos. LH [2015]7762, BS201503, and LH [2014]7222).

References

- [1] H. Li, Y. H. Xie, Q. Yang et al., "Cardioprotective effect of paeonol and danshensu combination on isoproterenol-induced myocardial injury in rats," *PloS One*, vol. 7, no. 11, Article ID e48872, 2012.
- [2] Y.-F. Ueng, Y.-H. Kuo, H.-C. Peng et al., "Diterpene quinone tanshinone IIA selectively inhibits mouse and human cytochrome p450A2," *Xenobiotica*, vol. 33, no. 6, pp. 603–613, 2003.
- [3] Y. Y. Wang, J. B. Zhu, L. Li, and Y. Jin, "Absorption and isolation of macroporous resin for five salvianolic acids from *Salviae miltiorrhizae*," *China Journal of Chinese Materia Medica*, vol. 33, no. 9, pp. 1004–1007, 2008.
- [4] S. Kan, J. Li, W. Huang, L. Shao, and D. Chen, "Microsphere resin chromatography combined with microbial bio-transformation for the separation and purification of salvianolic acid B in aqueous extract of roots of *Salvia miltiorrhiza* Bunge," *Journal of Chromatography A*, vol. 1216, no. 18, pp. 3881–3886, 2009.
- [5] M. Zhang, H. Yang, X. Chen et al., "In-situ extraction and separation of salvianolic acid B from *Salvia miltiorrhiza* Bunge by integrated expanded bed adsorption," *Separation and Purification Technology*, vol. 80, no. 3, pp. 677–682, 2011.
- [6] J.-C. Zhou, D.-W. Feng, and G.-S. Zheng, "Extraction of sesamin from sesame oil using macroporous resin," *Journal of Food Engineering*, vol. 100, no. 2, pp. 289–293, 2010.
- [7] L. Kavan, J. Rathouský, M. Grätzel, V. Shklover, and A. Zukal, "Surfactant-templated TiO₂ (anatase): characteristic features of lithium insertion electrochemistry in organized nano-structures," *The Journal of Physical Chemistry B*, vol. 104, no. 50, pp. 12012–12020, 2000.
- [8] J. Zhao, T. Wu, K. Wu, K. Oikawa, H. Hidaka, and N. Serpone, "Photoassisted degradation of dye pollutants. 3. Degradation of the cationic dye rhodamine B in aqueous anionic surfactant/TiO₂ Dispersions under visible light irradiation: evidence for the need of substrate adsorption on TiO₂ Particles," *Environmental Science & Technology*, vol. 32, no. 16, pp. 2394–2400, 1998.
- [9] S. Paria and K. C. Khilar, "A review on experimental studies of surfactant adsorption at the hydrophilic solid-water interface," *Advances in Colloid and Interface Science*, vol. 110, no. 3, pp. 75–95, 2004.
- [10] P. A. Kralchevsky, K. D. Danov, G. Broze, and A. Mehreteab, "Thermodynamics of ionic surfactant adsorption with account for the counterion binding: effect of salts of various valency," *Langmuir*, vol. 15, no. 7, pp. 2351–2365, 1999.
- [11] R. Atkin, V. S. J. Craig, E. J. Wanless, and S. Biggs, "Mechanism of cationic surfactant adsorption at the solid-aqueous interface," *Advances in Colloid and Interface Science*, vol. 103, no. 3, pp. 219–304, 2003.
- [12] Y. Li, N.-H. Lee, E. G. Lee, J. S. Song, and S.-J. Kim, "The characterization and photocatalytic properties of mesoporous rutile TiO₂ powder synthesized through self-assembly of nano crystals," *Chemical Physics Letters*, vol. 389, no. 1-3, pp. 124–128, 2004.
- [13] J. Gao, F. Guan, Y. Zhao et al., "Preparation of ultrafine nickel powder and its catalytic dehydrogenation activity," *Materials Chemistry and Physics*, vol. 71, no. 2, pp. 215–219, 2001.
- [14] F. A. M. Kang, F. Borges, C. Guimarães, J. L. F. C. Lima, C. Matos, and S. Reis, "Phenolic acids and derivatives: studies on the relationship among structure, radical scavenging activity, and physicochemical parameters," *Journal of Agricultural and Food Chemistry*, vol. 48, no. 6, pp. 2122–2126, 2000.
- [15] M. Kang, "The superhydrophilicity of Al-TiO₂ nanometer sized material synthesized using a solvothermal method," *Materials Letters*, vol. 59, no. 24-25, pp. 3122–3127, 2005.
- [16] Y. Yuan, J. Ding, J. Xu, J. Deng, and J. Guo, "TiO₂ nanoparticles co-doped with silver and nitrogen for antibacterial application," *Journal of Nanoscience and Nanotechnology*, vol. 10, no. 8, pp. 4868–4874, 2010.
- [17] K. S. W. Sing, D. H. Everett, R. A. W. Haul et al., "Reporting physisorption data for gas/solid systems with special reference to the determination of surface area and porosity (Recommendations 1984)," *Pure and Applied Chemistry*, vol. 57, no. 4, pp. 603–619, 1985.
- [18] Q. Yang, X. L. Zhang, X. Y. Li et al., "Coupling continuous ultrasound-assisted extraction with ultrasonic probe, solid-phase extraction and high-performance liquid chromatography for the determination of sodium Danshensu and four tanshinones in *Salvia miltiorrhiza* bunge," *Analytica Chimica Acta*, vol. 589, pp. 231–238, 2007.
- [19] X. Gong, S. Wang, and H. Qu, "Comparison of two separation technologies applied in the manufacture of botanical

- injections: second ethanol precipitation and solvent extraction,” *Industrial & Engineering Chemistry Research*, vol. 50, no. 12, pp. 7542–7548, 2011.
- [20] C. Ruizhan, Z. Shouqin, Z. Yonghong, B. Helong, and M. Fanlei, “Ultrahigh pressure extraction of Danshensu,” *Transactions of the Chinese Society of Agricultural Engineering*, vol. 2008, no. 1, 2008.
- [21] B. Y. Lee, S. H. Park, M. Kang, S. C. Lee, and S. J. Choung, “Preparation of Al/TiO₂ nanometer photo-catalyst film and the effect of H₂O addition on photo-catalytic performance for benzene removal,” *Applied Catalysis A: General*, vol. 253, no. 2, pp. 371–380, 2003.

